INVESTIGATION OF A BENDING CORRECTED FORMING LIMIT SURFACE FOR FAILURE PREDICTION IN SHEET METALS

Alexander Barlo[1,3*], Niko Manopulo[2], Mats Sigvant[1,4], Benny Endelt[3], Kristoffer Trana[1]

[1]Volvo Cars Stamping Engineering, Olofström, Sweden
[2]AutoForm Engineering GmbH, Zürich, Switzerland
[3]Department of Materials and Production, Aalborg University, Aalborg, Denmark
[4]Department of Mechanical Engineering, Blekinge Institute of Technology, Karlskrona, Sweden

ABSTRACT: Ensuring process feasibility is a high priority in the automotive industry today. Within the CAE departments concerning the manufacturing of body components, one of the most important areas of interest is the accurate prediction of failure in components through Finite Element simulations. This paper investigates the possibility of introducing the component curvature as a parameter to improve failure prediction. Bending-under-tension specimens with different radii are used to create a Bending Corrected Forming Limit Surface (BC-FLS), and a test die developed at Volvo Cars, depicting production-like scenarios by exposing an AA6016 aluminium alloy blank to a stretch-bending condition with biaxial pre-stretching, is used to validate the proposed model in the commercial Finite Element code AutoForm^{TM} R8. The findings of this paper showed that the proposed BC-FLS approach performed well in the failure prediction of the test die compared to the already in AutoForm^{TM} R8 implemented max failure approach.

KEYWORDS: Sheet Metal Forming, Failure Prediction, Formability, Curvature Dependency

1 INTRODUCTION

In the automotive industry today, one of the top priorities is to ensure process feasibility. One of the areas where this is seen, is within the Computer Aided Engineering (CAE) departments concerning the design and manufacturing of body components. Over the past years, more complex lightweight materials, such as AHSS and aluminium alloys, have been introduced along with increased component complexity. One of the great challenges the automotive industry faces today in regard to ensuring process feasibility, is the accurate prediction of failure of parts during the engineering phase. Between different industries, the term 'failure' has different meanings, but within the stamping department at Volvo Cars, failure is defined as *the onset of necking*.

For the past decades, the standard way of predicting failure in sheet metal forming simulations has been to apply the Forming Limit Diagram (FLD) originally proposed by Keeler & Backofen [1]. As the research on formability of sheet metals has advanced, the FLD approach has at several occasions been proven to perform poorly e.g. for components experiencing non-linear strain paths, or components where the stamping operation includes bending over a sharp radius.

The latter case has been investigated by e.g. Barlo et al. [2] presenting an evaluation of the performance of the FLD and the Non-Linear Forming Limit Diagram for failure prediction in dual-phase steel and aluminium alloys exposed to bending under tension. This evaluation of the FLD showed that it was indeed not able to accurately predict the onset of necking in a numerical model of the tested components.

Based on these observations, this paper aims to investigate how a bending correction of the standard Forming Limit Curve (FLC) could aid in the accurate failure prediction of components exposed to bending under tension for components of an AA6016 aluminium alloy.

2 EXPERIMENTAL WORK

In this paper two different experimental setups are used other than the Nakajima test setup used to determine the standard FLC:

* Corresponding author: Bruksgatan 1, SE-293 38 Olofström, Sweden, Alexander.Barlo@volvocars.com

1. Bending-under-tension experimental setup
2. Volvo Cars bending-under-tension test die

2.1 BENDING-UNDER-TENSION EXPERIMENTAL SETUP

The bending-under-tension experiments are used to perform the bending correction of the FLC. An experimental setup with three changeable double-curved punches with three different major radii of 3, 6, and 10 mm, and a minor punch radius of 100 mm is used. The reasoning for applying double-curved punches is to reduce the risk of a stochastic fracture location, and for the same reason the punch centre has been offset 6 mm to one side. An illustration of the experimental setup is presented in Figure 1.

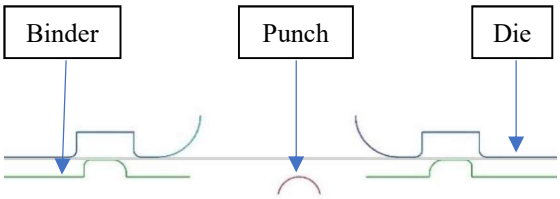

Fig. 1 *Illustration of the bending-under-tension experimental setup. The punch in the setup is changeable between punches of 3, 6, or 10 mm.*

To ensure the stretch-bending condition being present, locking beads (see Figure 2) are used to prevent material flow towards the area exposed to the actual bending operation.

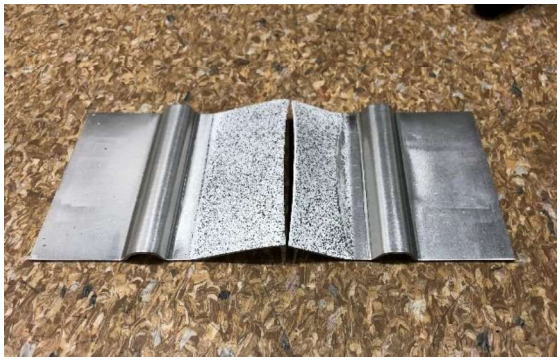

Fig. 2 *Post operation bending-under-tension specimen. The stochastic pattern applied to the surface is used for the DIC analysis.*

The experiments are performed in a single-action mechanical press using the die as the displacing tool, and with a ram velocity of 25 mm/s. The actual experimental setup is presented in Figure 3.

Fig. 3 *Setup for the bending-under-tension experiments.*

On top of the die, two cameras are mounted enabling 3D Digital Image Correlation (DIC) and strain history analysis through the software ARAMIS^{TM} developed by GOM.

2.2 VOLVO CARS BENDING-UNDER-TENSION TEST DIE

The Volvo Cars Bending-Under-Tension Test Die has been developed to depict a more production-like scenario, as the blank during stamping is exposed to a stretch-bending condition with biaxial pre-stretching as encountered in critical features such as door handles or fenders.

Fig. 4 *Volvo Cars Bending-Under-Tension Test Die panel. The die produces two different geometries, using punch nose radii of 4 and 8 mm.*

The panel produced by the test die is presented in Figure 4. The die produces two different geometries, and each geometry is repeated two times – one time with punch nose radius 4 mm and one with punch nose radius 8 mm. Furthermore, each of the geometries are then repeated a number of times with different feature depths to capture the actual forming limits. For the validation of the proposed failure prediction approach, only one of the geometries is initially of interest.

No DIC measurements has been recorded on this panel, why a manual inspection has been performed instead. The outcome of the manual inspection is presented in Figure 5.

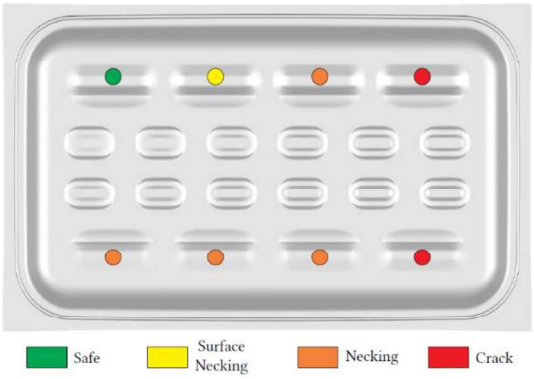

Fig. 5 *Outcome of the manual inspection of the stamped panel. Results for only one geometry is presented as this is initially the only one used for failure prediction approach validation.*

3 MATERIAL CHARACTERIZATION

For a validation of the proposed failure prediction approach, a numerical model of the Volvo Cars Bending-Under-Tension Test Die will be applied.

Table 1: *Material parameters for de modelling of the AA6016 aluminium alloy with the BBC05 yield surface.*

Material Parameter	Value	Unit
R_0	0.732	-
R_{45}	0.535	-
R_{90}	0.677	-
R_b	1.007	-
σ_0	110.3	MPa
σ_{45}	105.9	MPa
σ_{90}	106.5	MPa
σ_b	98.3	MPa
M	5.7	-

To ensure valid numerical results, an important factor is the applied material model. As experience throughout the years at Volvo Cars have shown the BBC05 material model to perform well, this material model will also be applied in this case. Material parameters of the AA6016 aluminium alloy used for the material model are listed in Table 1, and the applied hardening curve is presented in Figure 6.

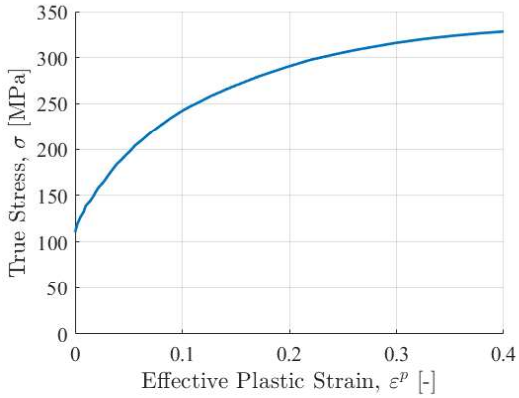

Fig. 6 *Hardening curve of the AA6016 aluminium alloy.*

4 DETERMINING THE EXPERIMENTAL ONSET OF NECKING

As defined in the introduction of this paper, the term failure is defined as onset of necking. Approaches to determine the onset of necking in experiments is something that has been discussed for several years and has still not been defined. Several approaches have been proposed e.g. the time dependent method proposed by Volk et al. [3] and a major strain rate based method proposed by Sigvant et al. [4]. To determine the initial FLC for onset of necking, as well as the onset of necking in the bending-under-tension experiments, an approach based on the development of the first derivative with respect to time of the major strain ($\dot{\varepsilon}_1$) proposed by Sigvant et al. [4] is applied. The major strain rate is calculated based on a statistical area introduced to the DIC measurement. The derivative is found using both the previous and next point in time as presented in Equation (1).

$$\dot{\varepsilon}_1 = \frac{\varepsilon_1(t_{n+1}) - \varepsilon_1(t_{n-1})}{t_{n+1} - t_{n-1}} \quad (1)$$

Figure 7 presents an example of how this analysis could turn out. In the method applied, the onset of necking is defined to occur when the maximum measured major strain rate exceeds the predicted average plus three standard deviations.

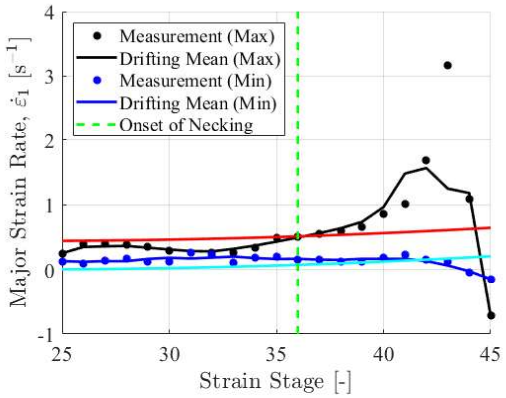

Fig. 7 *Illustration of determination of the onset of necking in a bending-under-tension R6 specimen. The onset of localized necking is passed once the drifting mean exceeds the predicted average (red line) plus three standard deviations.*

5 INFLUENCE OF BENDING ON SHEET FORMABILITY

The influence of bending on the formability of sheet materials is something that has been previously investigated by e.g. Atzema et al. [5] and Vallellano et al. [6]. A format often used to visualize the bending effect on sheet formability is to consider the outer surface maximum major strain at maximum force as a function of the thickness / tool radius ratio (α). Performing this check for the AA6016 aluminium alloy bending-under-tension experiments, Figure 8 show an increase in failure strain with the decrease of tool radius.

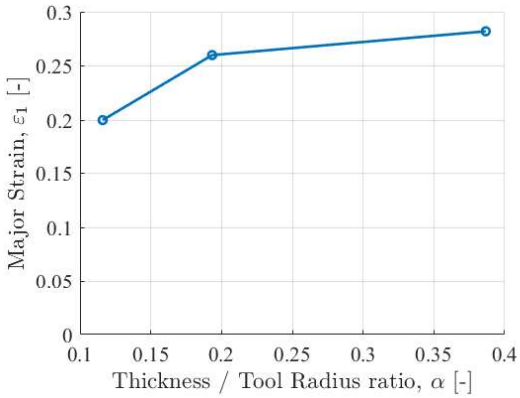

Fig. 8 *Bending influence on the outer surface maximum major strain for the AA6016 aluminium alloy bending-under-tension experiments. The values have been obtained from the DIC analysis.*

The increase of the major strain at the outer surface with a decrease in tool radius illustrates quite well why the FLD performs poorly for bending over sharp radii. The Nakajima test used to determine the standard FLC employs a hemispherical punch with a radius of 50 mm. With this observation, a bending correction of the standard FLC now seems even more interesting.

6 BENDING CORRECTION OF THE STANDARD FLC

In this first attempt to create a bending correction in this paper, the entire FLC will be corrected by an offset ($\Delta\varepsilon_1$). To determine this offset, the DIC measurements of the bending-under-tension experiments are used to find the delta value between the outer surface maximum major strain, and the standard FLC. This delta value is determined as presented in Equation (2) and illustrated in Figure 9.

$$\Delta\varepsilon_1 = \varepsilon_{1,DIC,max} - \varepsilon_{1,FLC}(\varepsilon_{2,DIC}) \qquad (2)$$

Table 2 presents a nomenclature of the variables presented in Equation (2), and Table 3 presents the data determined from the DIC measurements of the bending-under-tension experiments. Using Equation (2) the bending corrected curves are determined and presented in Figure 10. The idea of creating a bending corrected FLC has previously been presented by e.g. Ertürk et al. [7] proposing a bending correction of the FLC in the membrane layer of a numerical model.

Table 2: *Nomenclature of variables used in Equation (2).*

Variable	Definition	Unit
$\varepsilon_{1,DIC,max}$	Experimental global maximum major strain	-
$\varepsilon_{2,DIC}$	Experimental minor strain at $\varepsilon_{1,DIC,max}$	-
$\varepsilon_{1,FLC}(\varepsilon_{2,DIC})$	FLC limit strain at $\varepsilon_{2,DIC}$	-

Table 3: *Values necessary to calculate the $\Delta\varepsilon_{11}$ values for the bending correction.*

Radius	$\varepsilon_{1,DIC,max}$	$\varepsilon_{2,DIC}$	$\varepsilon_{1,FLC}(\varepsilon_{2,DIC})$
3	0.282	0.022	0.173
6	0.260	0.011	0.175
10	0.200	0.001	0.185

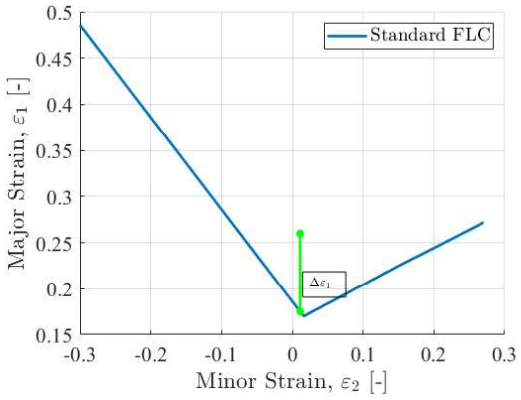

Fig. 9 *Illustration of the determination of the $\Delta\varepsilon_{11}$ value. The illustration exemplifies the R6 experiment, and the values presented in Table 3 have been used.*

To determine when to use which of the in Figure 10 presented curves, an additional parameter is introduced. In the work presented by Atzema et al. [4] the curvature (κ) on the concave side of the bend (tool curvature) was used as a measure to distinguish between the limit curves. This paper introduces the curvature to distinguish between limit curves, and thereby creating a limit surface. This surface will be called the Bending Corrected Forming Limit Surface (BC-FLS).

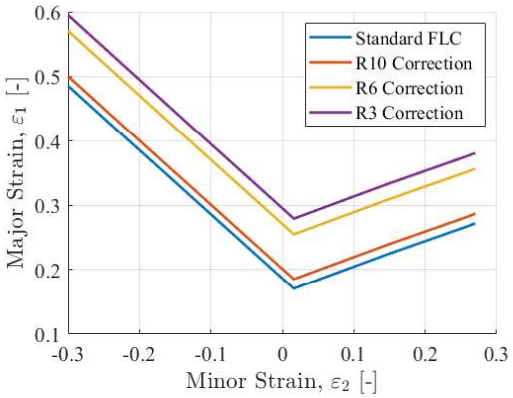

Fig. 10 *Bending corrected forming limit curves of the AA6016 aluminium alloy.*

As in [4], the curvature of the bend will be defined on the concave side i.e. it is calculated directly from the tool radius as presented in Equation (3)

$$\kappa = \frac{1}{R} \tag{3}$$

where R is the tool radius. This definition of the curvature yields the values presented in Table 4. The introduction of the curvature transfers the two-dimensional FLC into the three-dimensional space. A polynomial fitting of a surface to the data points, based on the best fit method, a BC-FLS ($\varepsilon_f(\varepsilon_{22}, \kappa)$) is performed, and yields a surface with an adjusted R^2 value of 0.9690. This limit surface is presented in Figure 11.

Table 4: *Curvature values at the concave side of the bend of the bending-under-tension specimens as well as for the Nakajima test.*

Radius:	3	6	10	50
Curvature:	0.3333	0.1667	0.1	0.02

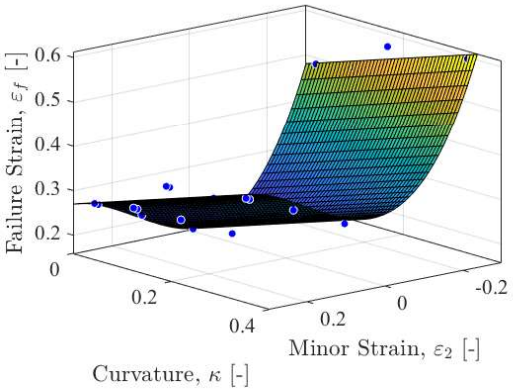

Fig. 11 *Bending corrected forming limit surface of the AA6016 aluminium alloy. The surface is created from a combination of the curves presented in Figure 10 and the curvatures presented in Table 4.*

The created BC-FLS does however have its limitations. Since the surface is fitted to data points, the presented failure strain definition should not be used outside of the experimentally defined space i.e. when the data points do not satisfy the conditions $-0.3 \leq \varepsilon_2 \leq 0.3$ and $0 \leq \kappa \leq 0.35$.

7 NUMERICAL EVALUATION

To validate the proposed BC-FLS approach, a numerical model of the Volvo Cars Bending-Under-Tension Test Die is used. The model is run in the commercial Finite Element code AutoForm™ R8. The model is created using the Elasto-Plastic Shell (EPS) element formulation with 11 integration points through the thickness, as well as an active consideration of surface pressure as a result of tool reactions and binder pressure. A simple friction model is applied using a global Coulomb friction coefficient of 0.12.

In this model, the draw beads have been of significance to ensure the presence of the stretch-bending phenomenon. Therefore, to reduce material flow in the model geometrical draw beads have been used.

To increase the possibility of capturing the onset of necking in the numerical model, a fine mesh is

applied in the zones exposed to bending with a minimum element size of 0.62 mm and a maximum allowed element angle of 10°.

To assess the state of the elements in the models, the idea of failure measure (F) to each element is introduced. The idea of failure in this model, is a direct relationship between the failure strain ($\varepsilon_f(\varepsilon_2, \kappa)$, graphically presented in Figure 11) and the element major strain at the convex side of the bend (ε_1) as presented in Equation (4). Once the failure measure reaches unity, the onset of necking has been reached for the element.

$$F = \frac{\varepsilon_1}{\varepsilon_f(\varepsilon_2, \kappa)} \tag{4}$$

Having a numerical model of the component, additional options regarding the definition of the curvature have become available. Evaluating the component at the convex side of the bended zones, the curvature is also found at this point. As the curvature could possibly variate within a single element, as exemplified in Figure 12, a choice must be made on which curvature definition should be used for the validation. As previously presented in Figure 8, the failure strain increases with an increase in curvature but due to the definition of the curvature on the concave side of the bend in the creation of the BC-FLS, the curvatures are lower than they should be from the DIC surface measurement. An initial attempt to account for this is to use the mean curvature (as defined in Equation (5)) of the element, thereby also lowering the curvature used for the validation.

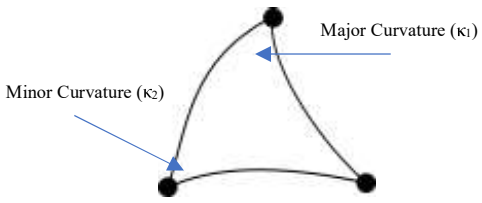

Fig. 12 *Example of curvatures on a triangular shell element. The indicated minor and major curvatures are used to calculate the mean curvature in the FE model used for the validation of the BC-FLS approach.*

$$\text{Mean Curvature} = \frac{\kappa_1 + \kappa_2}{2} \tag{5}$$

Having defined the curvature to be used in the numerical model, the validation can be performed. For the purpose of visualising the BC-FLS approach, Equation (4) has been implemented as a User Defined Variable (UDV) in AutoForm™ R8. Figures 13 (a) and (b) present the top and bottom rows of the Volvo Car Bending-Under-Tension Test Die component respectively.

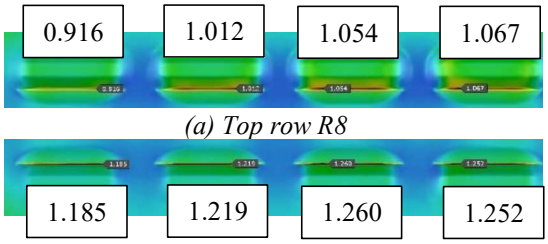

(a) Top row R8

(b) Bottom row R4

Fig. 13 *Local failure maxima for one geometry.*

The fringe plots presented for the two rows are so-called 'out of range' plots, meaning all elements having passed a certain threshold are presented without colour. In the case of the BC-FLS the threshold value is set to 1, resulting in all elements having passed the onset of necking is presented without colour in the fringe plots. The results presented seems to accurately predict the failure state observed in the manual inspection of the panel presented in Figure 5.

To support a claim of this application to perform better than the standard FLD, the Max Failure approach implemented in AutoForm™ R8 is used as a reference. The local max failure maxima are presented in Figures 14 (a) and (b).

Comparing the results from Figures 13 and 14, it can be seen that the proposed BC-FLS approach predicts the onset of necking more accurately than the Max Failure approach implemented in AutoForm™ R8.

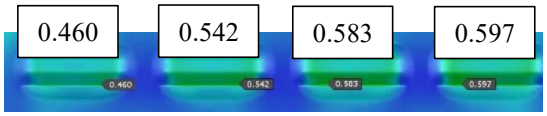

(a) Top row R8

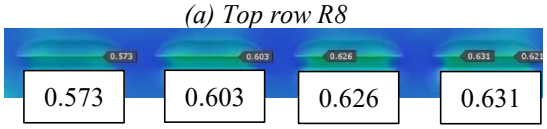

(b) Bottom row R4

Fig. 14 *Local max failure maxima for one geometry.*

8 CONCLUSIONS

This paper presented an approach for failure prediction in sheet metal components exposed to bending over sharp radii during the forming operation. This approach is based on performing a bending correction of the standard Forming Limit Curve (FLC) based on tool curvature, thereby transforming the standard Forming Limit Diagram (FLD) into a Bending Corrected Forming Limit Surface (BC-FLS). The surface was created using experimental data from a series of bending-under-tension tests, where global maximum strain values were used to correct the FLC. From these corrected curves, and the major punch curvature, the BC-FLS

was fitted using a best fit approach. An evaluation of the Volvo Cars Bending-Under-Tension Test Die with an AA6016 aluminium alloy blank was performed in the commercial Finite Element code AutoForm™ R8.

The numerical model validated the proposed failure prediction approach, and a comparison of the proposed approach and the already implemented Max Failure approach in AutoForm™ R8 aided to support the claim that the BC-FLS is a step towards a more accurate failure prediction of components exposed to bending-under-tension.

9 FUTURE WORK

The work presented in this paper, is at an early stage why several points of improvements can be pointed out. In its current form, the BC-FLS approach presented in this paper, is a post-processing tool. For the Volvo Cars Bending-Under-Tension Test Die component, the maximum failure (failure as defined by Equation (4)) is fortunately located at the very end of the simulation. However, scenarios of changing strain paths during one or multiple stamping operations could cause onset of necking at an arbitrary point in the process time without the user noticing it. Based on this, the first improvement that must be done to the approach is to introduce the principle of a process maximum failure, where the maximum failure obtained in a specific element is kept, even if this is reduced due to changes in strain paths.

Also, the bending correction of the FLC must be improved. As presented in Table 1, the major strains used for the bending correction is in very near proximity of the plain strain loading condition. During their investigation Atzema et al. [4] concluded that the effect of an increased curvature was close to negligible in the proximity of the uniaxial loading condition, moderate in the proximity of the biaxial loading condition and large in the proximity of the plain strain loading condition. This indicates that the bending corrected curves presented in Figure 10, and the BC-FLS presented in Figure 11, heavily overpredict the failure strain limit on parts of the left-hand side of the FLD, while a moderate overestimation is suspected to be present on parts of the right-hand side.

As presented in this paper, the BC-FLS approach has performed well for the Volvo Cars Bending-Under-Tension Test Die with an AA6016 aluminium alloy blank. To verify the approach as being general, the study must initially be extended to investigate multiple grades of aluminium and eventually also to include other material types e.g. dual-phase steel alloys.

REFERENCES

[1] Keeler S. & Backofen W.: *Plastic Instability and Fracture in Sheet Stretched over Rigid Punches*. In: ASM Trans. Quart **56**, 25-48, 1964.

[2] Barlo A., Sigvant M., & Endelt B.: *On the Failure Prediction of Dual-Phase Steel and Aluminium Alloys Exposed to Combined Tension and Bending*. In: The 38th International Deep Drawing Research Group Annual Conference, 2019.

[3] Volk W., Weiss H., Jocham D., & Suh J.: *Phenomenological and Numerical Description of Localized Necking using Generalized Forming Limit Concept*. In: 2013 IDDRG Conference Proceedings, 2013.

[4] Sigvant M., Mattiasson K. & Larsson M.: *The Definition of Incipient Necking and its implication on Experimentally or Theoretically Determined Forming Limit Curves.* In: 2008 IDDRG Conference Proceedings, 2008.

[5] Atzema E. H., Frictorie E., van den Boogard A. H. & Droog J. M. M.: *The Influence of Curvature on FLCs of Mild Steel, (A)HSS and Aluminium.* In: The 28th International Deep Drawing Research Group Annual Conference, 519-528, 2010.

[6] Vallellano C., Morales D., Martinez A.J., & Garcia-Lomas F. J.: *On the use of the Concave-Side Rule and Critical-Distance Methods to Predict the Influence of Bending on Sheet-Metal Formability.* In: Int J Mater Form **3**, 1167-1170, 2010.

[7] Ertürk S., Sester M., & Selig M.: *Limitations of Forming Limit Diagrams: Consideration of Bending Strain, Surface and Edge Cracks.* In: FTF 2018 Conference Proceedings, 2018.